

# **Predicting the physical properties of sea ice from a simple microstructural model**

M. Ingham

School of Chemical & Physical Sciences, Victoria University of Wellington, PO Box 600,  
Wellington, New Zealand

## **Abstract**

A simple microstructural model of sea ice based on dc resistivity data is used to predict other physical properties of the ice. It is found that the model produces an excellent fit to the observed variation of thermal conductivity with temperature down to temperatures of about  $-20\text{ }^{\circ}\text{C}$  and, for brine volume fractions above about 5%, is also able to predict the dependence of permeability on brine volume fraction. The microstructural model also gives good predictions of the specific heat capacity below  $-3\text{ }^{\circ}\text{C}$ , and of the variation of the imaginary part of variation of the dielectric permittivity with frequency. The principal failures of the model - a significant underestimation of the specific heat capacity at temperatures above about  $-3\text{ }^{\circ}\text{C}$ , and a poor fit to the real part of the permittivity – are believed to arise, respectively, from the complexity of the melting process of sea ice at high temperature, and the inability to model the effects of space charge polarization.

## 1. Introduction

Sea ice is a complex mixture of solid ice, brine, salts and air. An understanding of the microstructure of this mixture and the manner in which it varies with temperature is crucial to gaining a full understanding of the physical properties of sea ice. In large part these properties are determined by the size, geometry and connectivity of brine pores in the solid ice matrix. Brine is initially trapped in pockets within the ice matrix during the formation of sea ice. These pores exist on a range of length scales but, in general, shrink as the ice cools, and expand and coalesce during spring warming when large connected networks can develop. The derivation of an analytical model of this process would be an important step towards a full understanding of the thermal evolution of sea ice properties and the manner in which sea ice interacts with, and impacts upon, the environment.

Jones et al. (2012) have recently presented a simple microstructural model based on measurements of the bulk electrical resistivity of sea ice using the cross-borehole technique (Ingham et al., 2008; Jones et al., 2010, 2011). The model has been developed to explain the manner in which the ratio of the bulk electrical resistivity of the sea ice to that of the brine in the pores (a ratio known as the formation factor,  $F$ ) varies with the brine volume fraction in the ice ( $\phi_b$ ). The bulk electrical resistivity of sea ice is anisotropic and the model is successful in explaining the variation of both the vertical and horizontal components of  $F$  with  $\phi_b$ .

Although enabling the derivation of a microstructural model, the electrical resistivity of sea ice does not in itself hold much interest. In this paper therefore the ability of this simple microstructural model to predict other physical properties of sea ice is investigated. Properties of particular interest are the thermal conductivity ( $k$ ) of sea ice, which controls the

exchange of heat between the oceans and the atmosphere (Pringle et al., 2007), and the permeability ( $II$ ) which effects both the fate of melt water and the supply of nutrients through the ice (Golden et al., 2007). Variation of the specific heat capacity of sea ice ( $c_{si}$ ) and recent measurements of the low frequency dielectric permittivity ( $\epsilon^*$ ) of sea ice (e.g. Ingham et al., 2012a,b) are also tested. Success in explaining measurements of these properties would greatly enhance confidence in the utility of the microstructural model in understanding the wider physical properties of sea ice.

The basic microstructural model presented by Jones et al. (2012) is first reviewed and analytic expressions for its evolution with temperature are developed. These are then used to calculate, in turn, predicted variations in  $k$ ,  $c_{si}$ ,  $II$  and  $\epsilon^*$ . In each case the model values are compared to measured values. In conclusion the success of the microstructural model in explaining these properties is reviewed and pointers given to where further developments are necessary.

## **2. The microstructural model**

The basic microstructural model developed by Jones et al. (2012) consists of a cubic unit cell of fixed side length  $a+b$  (Figure 1). Although the geometry is idealized there are three basic features of the model which are necessary to explain the measured variations of the vertical and horizontal formation factors with brine volume fraction. The vertical columns of brine (of cross-sectional area  $a^2$ ) provide a conductive path which is necessary to give the measured values of  $F_V$  – the vertical formation factor. Similarly, horizontal tubes of brine (of cross-sectional area  $ac$ ) give a low resistivity path horizontally which is necessary to yield the observed values of  $F_H$ . An isolated volume ( $d^3$ ) of brine helps to make up the total brine

volume fraction but does not contribute to conductive paths through the sea ice. Neither air bubbles nor the possible presence of solid salts are allowed for in the microstructural model.

Multiple measurements of the formation factor were made over several months in first-year columnar sea ice off the coast of Barrow, Alaska (Jones et al., 2010). These allowed the variation with temperature of the four parameters ( $a$ ,  $b$ ,  $c$  and  $d$ ) to be derived (Figure 2). As discussed by Jones et al. (2012) the values are all relative to the smallest derived value of  $a$  ( $a_o$ ). Although there is some scatter in the values, for temperatures above  $-7$  °C they essentially lie on smooth curves allowing suitable analytic expressions for the variations in these parameters with temperature to be found. The variations in  $a$  and  $c$  with temperature are found to be best represented by sums of exponentials

$$a / a_o = 2.038 \exp(0.09933 T) + 2.291 \exp(0.7374 T) \quad (1)$$

$$c / c_o = 0.05959 \exp(-0.01212 T) + 7.044 \exp(1.767 T) \quad (2)$$

where  $T$  is in °C. As  $a+b$  is a constant

$$b / a_o = 20.49234 - a / a_o \quad (3)$$

The best simple fit to the variation of  $d$  with temperature is given by the quadratic

$$d / a_o = 0.02832T^2 + 0.595T + 10.15 \quad (4)$$

The fit of these expressions to the measured values of  $a$ ,  $b$ ,  $c$  and  $d$  are shown by the smooth curves in Figure 2. Although the resistivity data on which the models derived by Jones et al. (2012) were based were all measured at temperatures above  $-7$  °C, it is assumed that expressions (1), (2) and (3) give reasonable values of  $a$ ,  $b$  and  $c$  down to at least  $-20$  °C. The validity of this assumption is discussed later. Expression (4) for the variation of  $d$  with temperature has a minimum value at a temperature of approximately  $-10.6$  °C. Below this temperature  $d$  is assumed to be constant at this value.

96

97 Equations (1)-(4) thus provide analytic expressions for the variation of  $a$ ,  $b$ ,  $c$  and  $d$  with  
 98 temperature. From the model microstructure (Figure 1) the brine volume fraction in the  
 99 structure is given by

$$100 \quad \phi_b = \frac{a^2(a+b) + 2abc + d^3}{(a+b)^3} \quad (5)$$

101 and the variation of  $\phi_b$  with temperature is therefore specified by (1)-(5). The measurements  
 102 reported by Jones et al. (2010) were made on columnar sea ice which had a near constant  
 103 salinity profile that subsequently evolved in the surface layers as brine drainage occurred in  
 104 the spring. Generally,  $\phi_b$  is taken as being dependent not only on temperature but also on the  
 105 salinity ( $S$ ) of the sea ice (Cox & Weeks, 1983). The expression given by these authors

$$106 \quad \phi_b = (1 - \phi_a) \frac{\rho_i S}{F_1(T) - \rho_i S F_2(T)} \quad (6)$$

107 where  $\phi_a$  is the volume fraction of air,  $\rho_i$  is the ice density in  $\text{gcm}^{-3}$  given by

$$108 \quad \rho_i = 0.917 - 1.403 \times 10^{-4} T \quad (7)$$

109 and  $F_1$  and  $F_2$  are given functions of temperature, gives broad agreement with values given  
 110 by (5) for salinities in the range 4-6 ‰ as reported by Jones (2011).

111

112 The analytical expressions for the variations of  $a$ ,  $b$ ,  $c$  and  $d$  with temperature given by (1)-(4)  
 113 in conjunction with basic physical properties of ice and brine now allow the variation with  
 114 temperature of other physical properties of sea ice to be predicted.

115

### 116 **3. Thermal conductivity**

117

The thermal conductivity of sea ice controls the conductive heat flux through the ice (Eicken, 2003). As ice thickens by conduction of heat away from the ice/water interface this influences both the growth rate and the equilibrium ice thickness. Measurements of the thermal conductivity of both Arctic and Antarctic first-year sea ice have been presented by Pringle et al. (2007) and used to develop a parameterization for thermal conductivity in terms of temperature, salinity and density of the ice. The data used by Pringle et al. (2007) are shown in Figure 3 and include also, particularly for higher temperatures, earlier measurements from Nazintsev (1964) and Lewis (1967).

In terms of the microstructural model proposed by Jones et al. (2012) the bulk thermal conductivity of the unit cell shown in Figure 1 can be readily calculated. For a uniform vertical temperature gradient there are four distinct parallel thermal paths through the cell:

- (i) a path, of length  $a+b$ , solely through the vertical column of brine;
- (ii) a path which passes through ice for a length  $a+b-c$  and across the horizontal tubes of brine of thickness  $c$ .
- (iii) A path which passes through the isolated volume of brine. A length  $d$  of this path is in the brine and length  $a+b-d$  in ice.
- (iv) A path, of length  $a+b$ , which is solely within ice.

If the thermal conductivities of brine and ice are denoted by  $k_b$  and  $k_i$  respectively, the thermal conductivities along each of these separate paths are

$$k_{(i)} = k_b \quad (8a)$$

$$k_{(ii)} = \frac{k_b k_i (a+b)}{k_b (a+b-c) + k_i c} \quad (8b)$$

$$k_{(iii)} = \frac{k_b k_i (a+b)}{k_b (a+b-d) + k_i d} \quad (8c)$$

$$k_{(iv)} = k_i \quad (8d)$$

The effective thermal conductivity of the unit cell is then given by taking these four paths in parallel weighted by their respective cross-sectional areas

$$k = \frac{k_{(i)}a^2 + k_{(ii)}2ab + k_{(iii)}d^2 + k_{iv}(b^2 - d^2)}{(a + b)^2} \quad (9)$$

Neither equations (8) nor (9) depend upon the actual value of  $a_o$ . Thus, given the variations with temperature of  $a$ ,  $b$ ,  $c$  and  $d$  from equations (1)-(4) and of the thermal conductivities of brine and ice as used by Pringle et al. (2007)

$$k_b = 0.523 + 0.013T \text{ Wm}^{-1}\text{K}^{-1} \quad (10)$$

$$k_i = 2.14 - 0.011T \text{ Wm}^{-1}\text{K}^{-1} \quad (11)$$

equation (9) may be used to calculate the variation of the thermal conductivity of sea ice with temperature as predicted by the model microstructure.

152

This variation is shown by the dashed line in Figure 3. It is clear that the values predicted by equation (9) underestimate the thermal conductivity at most temperatures. However, it was pointed out by Jones et al. (2012) that a limitation of their microstructural model is that all the brine residing outside the vertical channels and horizontal tubes is represented as being in a single pore of volume  $d^3$ . In reality this volume of brine, particularly at lower temperatures, is distributed between multiple smaller pores. Jones et al. (2012) noted that as the sea ice warms, as well as there being changes in the dimensions of the connected channels and tubes, smaller pores expand and coalesce leading to fewer, larger, isolated pores (e.g. Light et al., 2003). In terms of the electrical resistivity data upon which the microstructural model is based a change in the number of isolated pores does not affect the bulk resistivity which is controlled by the conducting paths provided by the connected channels and tubes of brine.

The same is not true of the thermal conductivity. If the volume of brine  $d^3$  in the isolated pore is divided among  $n^3$  pores each of volume  $(d/n)^3$  then (8c) becomes

$$k_{(iii)} = \frac{k_b k_i (a + b)}{k_b (a + b - d/n) + k_i d/n} \quad (12)$$

At the temperatures of interest  $k_i$  is significantly greater than  $k_b$ . Thus increasing  $n$  has the effect of increasing  $k_{(iii)}$  and through this the overall thermal conductivity  $k$ . Using a purely empirical variation of  $n$  with  $T$  of

$$n = 1.7314 - 0.3145T \quad (13)$$

- implying that the number of isolated pores between which the volume  $d^3$  of brine is divided decreases from about 500 at  $-20^\circ\text{C}$  to about 100 at  $-10^\circ\text{C}$ , and to about 10 at  $-2^\circ\text{C}$  - gives the variation of thermal conductivity with temperature shown by the solid line in Figure 3. This is in excellent agreement with the measured values of the thermal conductivity of sea ice. The validity of (13) is discussed below.

#### 4. Specific heat capacity

The other thermal property of sea ice of interest is the specific heat capacity ( $c_{si}$ ). Field measurements of  $c_{si}$  date back to Malmgren (1927) and have also been reported by Nazintsev (1959, 1964) and Trodahl et al. (2000). On the basis of these Schwerdtfeger (1963) and Ono (1967) derived parameterisations for  $c_{si}$  in terms of temperature and salinity. That of Ono (1967)

$$c_{si} = 2113 + 7.5T - 3.4S + 0.084ST + 18040 \frac{S}{T^2} \quad (14)$$

where  $S$  is in  $\text{‰}$ ,  $T$  in  $^\circ\text{C}$ , and  $c_{si}$  in  $\text{J kg}^{-1} \text{K}^{-1}$  gives the curves shown in Figure 4 for salinities of 4, 5 and 6  $\text{‰}$ .



In terms of the microstructural model the specific heat capacity may be expressed as

$$c_{si} = \frac{\rho_b V_b c_b + \rho_i V_i c_i - L_i dm_i / dT}{\rho_b V_b + \rho_i V_i} \quad (15)$$

The first two terms in the numerator represent the energy required to raise the temperature of the brine and ice by 1 °C, while the third term accounts for melting of the essentially (pure) ice at the walls of pore spaces as the temperature rises. The denominator expresses the total mass of the unit cell in the microstructural model. Standard expressions exist for the variations of  $\rho_b$ ,  $\rho_i$ ,  $c_i$  and  $L_i$  with temperature (e.g. Eicken, 2003; Weeks, 2010),  $c_b$  as a function of temperature and salinity is given by Sharqawy et al. (2010), and  $V_b$  and  $V_i$  can be expressed in terms of the microstructural model dimensions. The rate at which ice melts at the boundaries of pores is

$$\begin{aligned} \frac{dm_i}{dT} = \frac{d}{dT}(\rho_i V_i) = & \frac{d\rho_i}{dT} \left( (a+b)^3 - a^2(a+b) - 2abc - d^3 \right) \\ & + \rho_i \left( -2a \frac{da}{dT} (a+b) - 2bc \frac{da}{dT} - 2ab \frac{dc}{dT} - 2ac \frac{db}{dT} - 3d^2 \frac{dd}{dT} \right) \end{aligned} \quad (16)$$

which may be expressed analytically using (1)-(4) and  $\rho_i(T)$ .

The predicted variation of  $c_{si}$  with temperature given by (15) is shown in Figure 4 by the solid line and shows good agreement with the experimental data at lower temperatures but significantly underestimates the sharp rise in  $c_{si}$  at temperatures above about -3 °C.

## 5. Permeability

The permeability ( $I$ ) of sea ice is important for a number of reasons. In the growth phase of sea ice it allows the desalination of ice and thus controls the flux of salt to the underlying ocean (e.g. Haarpaintner et al., 2001), while in the spring it has an effect on the formation and

drainage of melt ponds (Fetterer et al., 1998). Columnar sea ice is effectively impermeable for brine volume fractions below about 5% (Weeks & Ackley, 1986). The association of 5% brine volume fraction with typical ice temperatures and salinities of -5 °C and 5 ‰ has been termed the “rule of fives” by Golden et al. (1998). This observation, and potentially a critical transition at 5% brine volume fraction (Golden et al., 2007) are hinted at by the measured variation of permeability with brine volume fraction presented by Petrich et al. (2006) and shown in Figure 5.

More generally, the permeability of a porous medium and how it relates to fluid volume is of interest for reasons as diverse as oil recovery and groundwater studies. One of the earliest proposed relationships between  $\Pi$  and porosity ( $\phi$ ) was the Kozeny-Carmen equation (e.g. Scheidegger, 1974)

$$\Pi = \phi^3 / c \sigma^2 \quad (17)$$

where  $c$  is an empirical constant and  $\sigma$  is the pore surface area per unit volume. Relationships between permeability and the electrical formation factor  $F$  have long been assumed to exist because of the dependence of both on the pore geometry. Johnson et al. (1986) proposed one such relationship

$$\Pi = \Lambda^2 / 8F \quad (18)$$

which has since been derived on a theoretical basis by Avellaneda & Torquato (1991) and used by, for example, Revil & Florsch (2010) in attempts to derive a direct relationship between permeability and spectral induced polarization (SIP) measurements. In (18)  $\Lambda$  is the hydraulic pore radius.

The microstructural model allows the use of (18) to predict the variation of the permeability of sea ice with brine volume fraction. One estimate of  $\Lambda$  is to use the reciprocal of the pore

surface area per unit volume. Expressed in terms of  $a$ ,  $b$ ,  $c$  and  $d$ , and allowing for the same empirical variation in the number of isolated pore volumes given by (13),  $\Lambda$  is given by

$$\Lambda = \frac{a^2(a+b) + 2abc + d^3}{2(ac + 4bc) + 4ab + 2a(a+c) + 6nd^2} \quad (19)$$

Although it is the vertical permeability that is of interest, horizontal pore spaces are also included in this estimate as in bulk sea ice overall vertical connection will be through a network of both vertically and horizontally oriented pores. The inclusion of the isolated pores in (19) makes the estimated hydraulic pore radius a mean over all pores. As noted previously the brine volume fraction is given by (5) and this can in turn be related to the measured vertical formation factor  $F_V$  by

$$F_V = \phi_b^{-1.9681} \quad (20)$$

where -1.9681 is the gradient of the plot of  $\log F_V$  against  $\log \phi_b$  (see Jones et al. (2012) Fig. 1b) when constrained to give  $F_V = 1$  when  $\phi_b = 1$ .

Unlike equations (9) and (15), (19) is not independent of  $a_o$ . Thus, to use (5), (19) and (20) to calculate the variation of permeability with brine volume fraction it is necessary to choose a suitable value for this parameter. The choice of an appropriate value for  $a_o$  was discussed at length by Jones et al. (2012) who concluded that a value of 100  $\mu\text{m}$  was a suitable average. Using this value the variation of permeability with  $\phi_b$  calculated from the microstructural model is shown as the solid line in Figure 5 and, within the range  $5\% \leq \phi_b \leq 15\%$ , there is a reasonable fit to the measured values of permeability.

## 6. Dielectric permittivity

At GHz frequencies the dielectric permittivity of sea ice ( $\epsilon^*$ ) is of interest because of its relevance to remote sensing (Hallikainen & Winebrenner, 1992). At lower frequencies interest in  $\epsilon^*$  is related both to developing automated monitoring of sea ice salinity (Pringle et al., 2009) and to understanding sea ice microstructure (Ingham et al., 2012a). With this later aim Ingham et al. (2012a) have recently presented the results of *in-situ* measurements in first-year Antarctic sea ice of the horizontal component of  $\epsilon^*$  in the frequency range 10 Hz – 100 kHz. Measurements were made using a development of the cross borehole resistivity technique (Ingham et al., 2008). Similar results have recently been reported by Ingham et al. (2012b) for first-year landfast sea ice at Barrow, Alaska, and the variation with frequency of the real ( $\epsilon'$ ) and imaginary ( $\epsilon''$ ) parts of the relative permittivity at a temperature of -4 °C for these data is shown in Figure 6.

The imaginary part of the permittivity is largely controlled by ionic conduction through the brine (Buchanan et al., 2011). However, as reported by Ingham et al. (2012a) the real part shows a decrease at a frequency of some 10's of kHz which is related to dielectric relaxation of the ice lattice. At low frequency there is also a significant contribution to  $\epsilon'$  from the formation of electric double layers at pore surfaces and the effect of space charge polarization in the brine (Buchanan et al., 2011).

As for  $k$  and  $II$ , the analytic expressions for  $a$ ,  $b$ ,  $c$  and  $d$  as functions of temperature can be used to model the relative permittivity. The relative permittivity of columnar sea ice may be calculated from the microstructural model by first calculating the complex conductivity  $\sigma^*$ .

This is related directly to  $\epsilon^*$  by  $\sigma^* = i\omega\epsilon_0\epsilon^*$ . The horizontal component of the complex conductivity is

$$\begin{aligned} \sigma_H^* = & \frac{b(a+b-c)-d^2}{(a+b)^2} \sigma_{ice}^* + \frac{ac}{(a+b)^2} \sigma_{brine}^* \\ & + \frac{bc+a(a+b-c)}{(a+b)} \frac{\sigma_{ice}^* \sigma_{brine}^*}{b\sigma_{brine}^* + a\sigma_{ice}^*} \\ & + \frac{d^2}{(a+b)} \frac{\sigma_{ice}^* \sigma_{brine}^*}{(a+b-d)\sigma_{brine}^* + d\sigma_{ice}^*} \end{aligned} \quad (22)$$

where  $\sigma_{ice}^*$  and  $\sigma_{brine}^*$  are the frequency dependent complex conductivities of ice and brine.

These both take the form

$$\sigma^* = i\omega\epsilon_o \left\{ \epsilon_\infty + \frac{\epsilon_{DC} - \epsilon_\infty}{1 + i\omega\tau} \right\} + \sigma_{DC} \quad (23)$$

in which the first term represents the respective Debye relaxation of ice or brine and the second is the DC conductivity, which in the case of ice is effectively zero. Values for  $\epsilon_{DC}$ ,  $\epsilon_\infty$ , and the relaxation time  $\tau$  have been given for ice by, amongst others, Auty & Cole (1952), Evans (1965) and Johari & Whalley (1981); and for brine by Stogryn (1971) and Klein & Swift (1977). Taking the values given by Auty & Cole (1952) and Klein & Swift (1977) gives the model values for the real and imaginary parts of  $\epsilon^*$  at a temperature of -4 °C shown by the smooth curves in Figure 6.

293

It is clear that the model values significantly underestimate the measured values of  $\epsilon'$  at all frequencies and, in particular, do not show the rise that occurs in the measured values with decreasing frequency. In contrast, the microstructural model provides a good fit to the variation with frequency of  $\epsilon''$ , the imaginary part of the permittivity.

298

## 7. Discussion

300

From the results presented above it is clear that the microstructural model is successful in predicting both the thermal conductivity and the permeability of sea ice over reasonably large ranges of temperature and brine volume fraction. It is less successful in predicting the specific heat capacity at temperatures above  $-3^{\circ}\text{C}$ , and cannot account for the frequency variation of the real part of the dielectric permittivity.

The temperature range over which the variation in the parameters in the microstructural model was initially determined was from  $-7^{\circ}\text{C}$  to  $\sim -1^{\circ}\text{C}$ . The prediction of thermal conductivity and specific heat capacity to lower temperatures thus incorporate considerable extrapolation in the variation of the microstructural model dimensions with temperature. Light et al. (2003) have reported on the variation in the dimensions of brine inclusions with temperature and noted a continuous increase in dimensions with rising temperature from at least  $-15^{\circ}\text{C}$  to  $-2^{\circ}\text{C}$ . Thus, although future measurement of the bulk electrical resistivity at lower temperatures may lead to a refinement of the lower temperature variations of  $a$ ,  $b$ ,  $c$  and  $d$ , the extrapolation is not inherently unreasonable. The empirical variation with temperature in the number of isolated pores (13) is similarly qualitatively consistent with observations by Light et al. (2003) of a decrease in the number of brine inclusions with increasing temperature. Thus, notwithstanding the assumptions, the simple microstructural model given by Jones et al. (2012) does appear to be able to model the observed variation of thermal conductivity down to temperatures as low as  $-20^{\circ}\text{C}$ .

Although the extrapolation to lower temperature of the dimensions of the microstructural model appears reasonable, at temperatures above  $-2^{\circ}\text{C}$ , when the ice is in the advanced stages of melting, the variations in  $a$ ,  $b$ ,  $c$  and  $d$  are based on very few data points. The high temperature variations in the parameters should probably therefore be regarded as somewhat

tentative. Given this, although the microstructural model is successful in predicting the high temperature thermal conductivity, the complexity of the melting process, involving surface ablation and a decrease in surface salinity due to flushing with meltwater, means that it is perhaps unsurprising that it is less successful in predicting the high temperature specific heat capacity.

The fit of the model values to the bulk permeability is critically dependent on the choice of  $a_o$ . As is seen from Figure 6, the value of 100  $\mu\text{m}$  suggested by Jones et al. (2012) provides a good overall fit to the observational data, but possibly tends to underestimate permeability at brine volume fractions of about 10% and higher. Rather than considering an average value of  $a_o$  the bulk permeability may in reality be dominated by a smaller number of pores with larger cross-section. This can be accounted for by increasing the assumed value for  $a_o$  and leads to a higher model permeability. The lack of bulk resistivity measurements at lower than  $-7^\circ\text{C}$  means that any extrapolation of  $\Pi$  at brine volume fractions lower than 5%, where sea ice is believed to be impermeable, is tentative. If a transition to impermeability is related to a percolation transition as has been suggested (Golden et al., 1998, 2007) then it also implies a change in the basic microstructure which would make any such extrapolation to lower  $\phi_b$  invalid.

The misfit to the real part of the dielectric permittivity seen in Figure 7 is the most serious failure of the microstructural model to fit a measured physical property. This results largely from the effects of space charge polarization not being included in the microstructural model. Space charge polarization is the result of the formation of electric double layers at ice/brine interfaces and the separation of positive and negative charges in the brine under the influence of an AC electric field (e.g. MacDonald, 1953). The main effect is to produce the sharp rise

in  $\varepsilon'$  at low frequency. However, polarization within the brine at ice/brine interfaces can also modify the time constant of the principle dielectric relaxation. Thus the decrease in  $\varepsilon'$  with increasing frequency predicted by the microstructural model occurs almost one order of magnitude of frequency lower than in the observational data. Mathematically the contribution of space charge polarization to the overall bulk conductivity has represented by Buchanan et al. (2011) as a separate term  $K(i\omega)^m$  where  $K$  and  $m$  are temperature dependent. However, the incorporation of such effects into the physical model is non-trivial and requires much further work. In contrast, as the ionic conductivity is much greater than the effect of space charge polarization, the microstructural model does provide a good fit to the variation with frequency of  $\varepsilon''$ , the imaginary part of the permittivity.

In summary, the successful prediction of the bulk thermal conductivity and permeability of sea ice lends considerable support to the simple model presented by Jones et al. (2012) as a good first order representation of the microstructure of columnar sea ice and the way in which it varies with temperature. Additional measurements at temperatures below  $\sim -10^\circ\text{C}$  would help to justify the present extrapolation to lower temperatures, while improved prediction of the high temperature variation in specific heat capacity requires further measurements in the later stages of melting. Incorporation of the space charge polarization into the model is necessary to fully describe the complex permittivity.

## References

Auty, R. P. and R. H. Cole, 1952, Dielectric properties of ice and solid  $\text{D}_2\text{O}$ , *J. Chem. Phys.*, 20(8), 1309-1314.



376 Avellaneda, M. and S. Torquato, 1991, Rigorous link between fluid permeability, electrical  
377 conductivity and relaxation times for transport in porous media, *Phys. Fluids A*, 3 (11), 2529-  
378 2540.

379

380 Buchanan, S., M. Ingham and G. Gouws, 2011, The low frequency electrical properties of sea  
381 ice, *J. Appl. Phys.*, 110, 074908, doi:10.1063/1.3647778.

382

383 Cox, G. F. N. and W. F. Weeks, 1975, Brine drainage and initial salt entrapment in sodium  
384 chloride ice, *CRREL Res. Rep.*, 345.

385

386 Eicken, H., 2003, From the microscopic, to the macroscopic, to the regional scale: Growth,  
387 microstructure and properties of sea ice, in *Sea Ice: An Introduction to its Physics, Chemistry,*  
388 *Biology and Geology*, edited by D. N. Thomas and G. S. Dieckmann, pp. 22–81, Blackwell  
389 Sci., Oxford, U. K.

390

391 Evans, S., 1965, Dielectric properties of ice and snow –a review, *J. Glaciology*, 5, 773-792.

392

393 Fetterer, F. and N. Untersteiner, 1998, Observations of melt ponds on arctic sea ice, *J.*  
394 *Geophys. Res.*, 103 (C11), 24821-24835.

395

396 Golden, K. M., S. F. Ackley and V. I. Lytle, 1998, The percolation phase transition in sea ice,  
397 *Science*, 282, 2238-2241.

398

399 Golden, K. M., H. Eicken, A. L. Heaton, J. Miner, D. J. Pringle and J. Zhu, 2007, Thermal  
400 evolution of permeability and microstructure in sea ice, *Geophys. Res. Lett.*, *34*, L16501,  
401 doi:10.1029/2007GL030447.  
402

403 Haarpaintner, J., J. –C. Gascard and P. M. Haugan, 2001. Ice production and brine formation  
404 in Storfjorden, Svalbard, *J. Geophys. Res.*, *106* (C7), 14001-14013.  
405

406 Hallikainen, M. and D.P. Winebrenner, 1992, The physical basis for sea ice remote sensing,  
407 in *Microwave Remote Sensing of Sea Ice*, edited by F.D. Carsey, pp. 29-46, Geophysical  
408 Monograph, vol. 68, American Geophysical Union, Washington.  
409

410 Ingham, M., D. Pringle and H. Eicken, 2008, Cross-borehole resistivity tomography of sea  
411 ice, *Cold Reg. Sci. Tech.*, *52*, 263-277.  
412

413 Ingham, M., G. Gouws, S. Buchanan, R. Brown and T. Haskell, 2012a, In-situ measurements  
414 of the low frequency dielectric permittivity of first-year Antarctic sea ice, *Cold Reg. Sci.*  
415 *Tech.*, doi: 10.1016/j.coldregions.2012.07.008.  
416

417 Ingham, M., S. Buchanan, G. Gouws, H. Eicken and T. Haskell, 2012b, In-situ measurement  
418 of the low frequency permittivity of sea ice, Fall Meeting, American Geophysical Union, San  
419 Francisco, 3-7 December 2012.  
420

421 Johari, G. P. and E. Whalley, 1981, The dielectric properties of ice Ih in the range 272-133 K,  
422 *J. Chem. Phys.*, *75*(3), 1333-1340.  
423

424 Johnson, D. L., J. Koplik and L. M. Schwartz, 1986, New pore-size parameter characterizing  
425 transport in porous media, *Phys. Rev. Lett.*, 57, 2564-2567.  
426

427 Jones, K. A., 2011, Cross-borehole DC resistivity tomography of sea ice: temporal and spatial  
428 variations in the anisotropic microstructure, Unpublished PhD Thesis, School of Chemical &  
429 Physical Sciences, Victoria University of Wellington, New Zealand, pp 238.  
430

431 Jones, K. A., M. Ingham, D. J. Pringle and H. Eicken, 2010, Temporal variations in sea ice  
432 resistivity: resolving anisotropic microstructure through cross-borehole dc resistivity  
433 tomography, *J. Geophys. Res.*, 115, C11023, doi:10.1029/2009JC006049.  
434

435 Jones, K. A., M. Ingham, D. J. Pringle, D.J. and H. Eicken, 2011, Cross-borehole resistivity  
436 tomography of Arctic and Antarctic sea ice, *Annals. Glac.*, 52(57), 161-168.  
437

438 Jones, K. A., M. Ingham and H. Eicken, 2012, Modelling the anisotropic brine microstructure  
439 in first-year sea ice, *J. Geophys. Res.*, 117, C02005, doi:10.1029/2011JC007607.  
440

441 Klein, L. A. and C. T. Swift, 1977, An improved model for the dielectric constant of sea  
442 water at microwave frequencies, *IEEE Trans. Antenn. Prop.*, AP-25, 104-111.  
443

444 Lewis, E. L., 1967, Heat flow through winter ice, in *Physics of Snow and Ice: International*  
445 *Conference on Low Temperature Science 1966, vol. 1 (1)*, edited by H. Oura, pp. 611– 631,  
446 Inst. of Low Temp. Sci., Hokkaido Univ., Sapporo, Japan.  
447

448 Light, B., G. A. Makyut and T. C. Grenfell, 2003, Effects of temperature on the  
449 microstructure of first-year Arctic sea ice, *J. Geophys. Res.*, *108*, C2, 3051,  
450 doi:10.1029/2001JC000887.  
451  
452 MacDonald, J. R., 1953, Theory of ac space-charge polarization effects in photo conductors,  
453 semiconductors, and electrolytes, *Phys. Rev.*, *92*, 4-17.  
454  
455 Maksym, T. and M. O. Jefries, 2000, A one-dimensional percolation model of flooding and  
456 snow ice formation on Antarctic sea ice, *J. Geophys. Res.*, *105*(C11), 26313-26331.  
457  
458 Malmgren, F., 1927, On the properties of sea-ice, *Norwegian North Pole Expedition 'Maud'*  
459 *1918-1925, 1*, 1-67.  
460  
461 Nazintsev, Y. L., 1959, Eksperimental'noe opredelenie teploemkosti i tem-  
462 peraturoprovodnosti moskogo l'da (Experimental determination of the specific heat and  
463 thermometric conductivity of sea ice), *Probl. Arkt. Antarkt.*, *1*, 65-71.  
464  
465 Nazintsev, Y. L., 1964. Nekotorye dannye k raschetu teplovykh Svoistv morskogo l'da  
466 (Some data on the calculation of thermal properties of sea ice), *Tr. Arkt. Antarkt. Nauchlo*  
467 *Issled Inst.*, *267*, 31– 47.  
468  
469 Ono, N., 1967, Specific heat and fusion of sea ice, in *Physics of Snow and Ice: International*  
470 *Conference on Low Temperature science 1966*, edited by H. Oura. Institute of Low  
471 Temperature Science, Hokkaido University, Sapporo, Japan.  
472

473 Ono, N. and T. Kasai, 1985, Surface layer salinity of young sea ice, *Ann. Glaciol.* 6, 298-299.  
474

475 Petrich, C., P. J. Langhorne and Z. F. Sun, 2006, Modelling the interrelationships between  
476 permeability, effective porosity and total porosity in sea ice, *Cold Reg. Sci. Tech.*, 44, 131-  
477 144.  
478

479 Pringle, D.J., H. Eicken, H. J. Trodahl and L. G. E. Backstrom, 2007, Thermal conductivity  
480 of landfast Antarctic and Arctic sea ice, *J. Geophys. Res.*, 112, C04017,  
481 doi:10.1029/2006JC003641.  
482

483 Pringle, D., G. Dubois and H. Eicken, 2009, Impedance measurements of the complex  
484 dielectric permittivity of sea ice at 50 MHz: pore microstructure and potential for salinity  
485 monitoring, *J. Glaciology*, 55, 81-94.  
486

487 Revil, A. and N. Florsch, 2010, Determination of permeability from spectral induced  
488 polarization in granular media, *Geophys. J. Int.*, 181, 1480-1498.  
489

490 Saeki, H., T. Takeuchi, M. Sakai and E. Suenaga, 1986, Experimental study on permeability  
491 coefficients of sea ice, in: *Proceedings of 1<sup>st</sup> International Conference on Ice Technology*,  
492 editors Murthy, T.K.S., Connor, J.J. & Brebbia, C.A., Springer-Verlag, Berlin, pp237-246.  
493

494 Saito, T. and N. Ono, 1978, Percolation of sea ice. I – Measurements of kerosene  
495 permeability of NaCl ice, *Low Temp. Sci. Ser. A*, 37, 55-62.  
496

497 Scheidegger, A. E., 1974, The Physics of Flow Through Porous Media, University of Toronto  
498 Press, Toronto.

499

500 Schwerdtfeger, P., 1963, The thermal properties of sea ice, *J. Glaciol.*, 4, 789-807.

501

502 Sharqawy, M. H., V. J. H. Lienhard and S. M. Zuabair, 2010, Thermophysical properties of  
503 seawater: A review of existing correlations and data, *Desalination and Water Treatment*, 16,  
504 354-380.

505

506 Stogryn, A., 1971, Equations for calculating the dielectric constant of saline water, *IEEE*  
507 *Trans. Microwave Theory Tech.*, MTT-19, 733-736.

508

509 Trodahl, H. J., M. McGuinness, P. Langhorne, K. Collins, A. Pantola, I. Smith and T. Haskell,  
510 2000, Heat transport in McMurdo Sound first-year fast ice, *J. Geophys. Res.*, 105, 11,347-  
511 11,358.

512

513 Weeks, W. F., 2010, On Sea Ice, University of Alaska Press, Fairbanks, Alaska.

514

515 Weeks, W. F. and S. F. Ackley, 1986, The growth, structure, and properties of sea ice, in: *The*  
516 *Geophysics of Sea Ice*, editor N. Untersteiner, NATO ASI Series, Series B: Physics, vol 146.  
517 Plenum Press, New York, NY, USA, pp. 9-164.

518

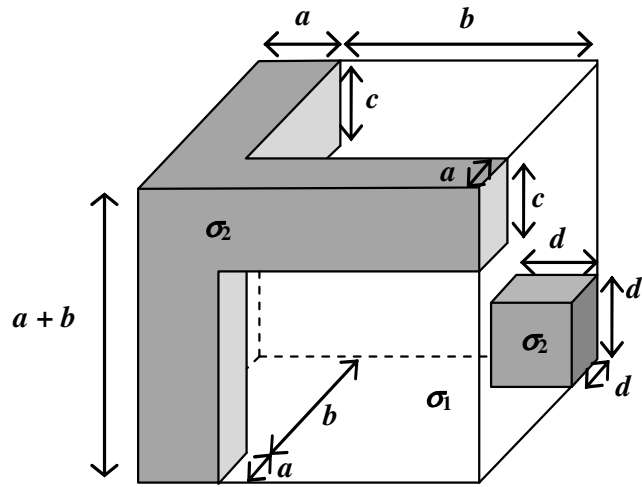


Figure 1: The microstructural model presented by Jones et al. (2012). Shaded regions represent brine channels/pores with conductivity  $\sigma_2$ , while unshaded regions of conductivity  $\sigma_1$  represent the ice matrix.

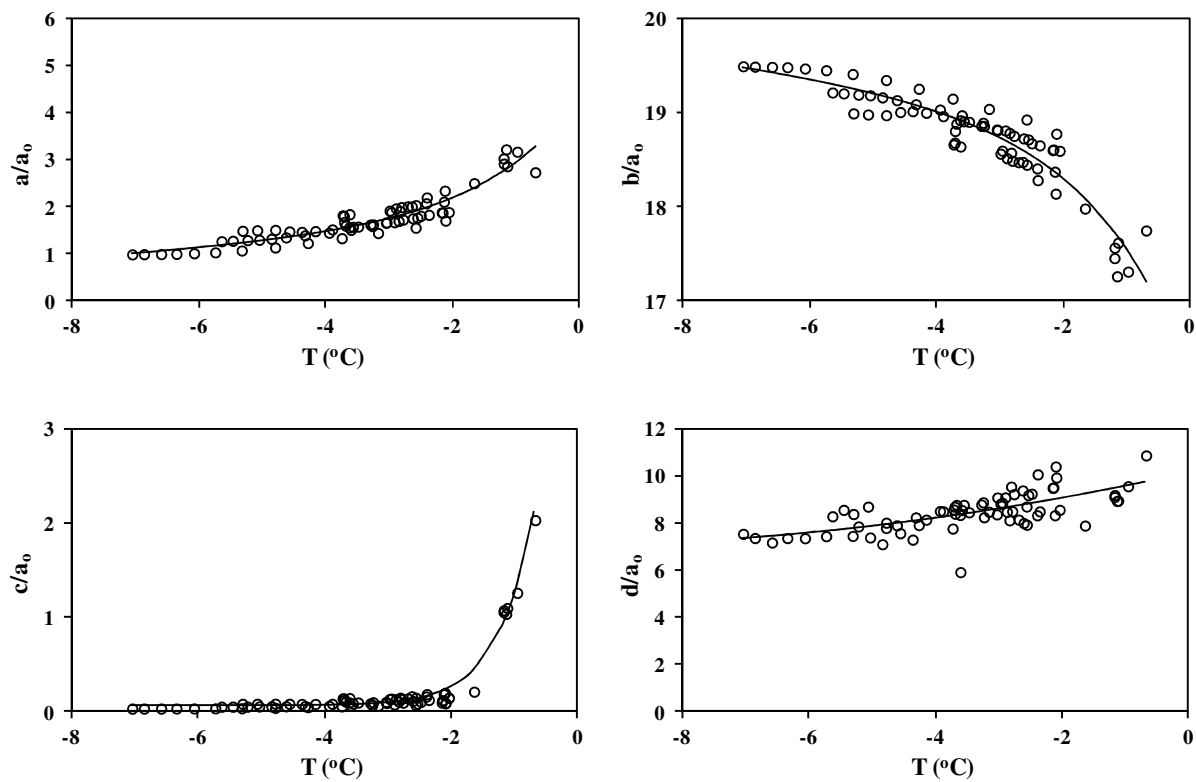


Figure 2: Fits of analytic functions of temperature to the parameters  $a$ ,  $b$ ,  $c$  and  $d$  in the microstructural model. All dimensions are relative to a value  $a_0$ .



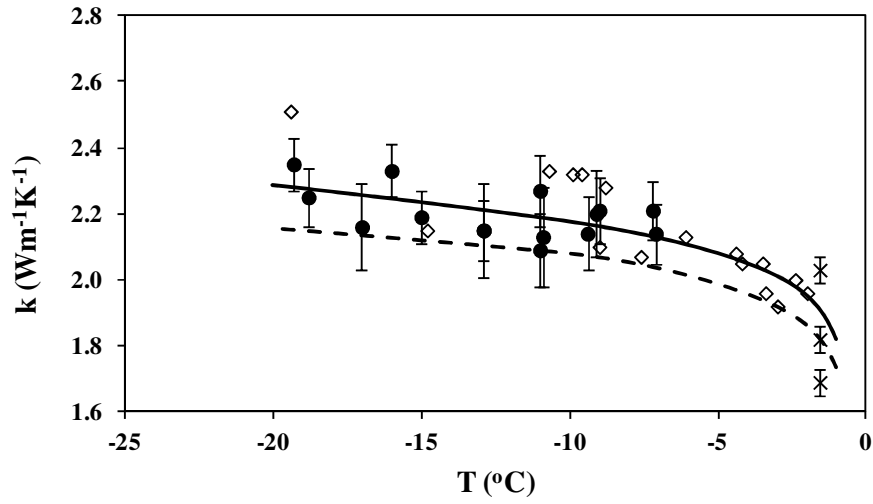


Figure 3: Variation of thermal conductivity with temperature predicted by the microstructural model compared to measured values. Solid line – predicted thermal conductivity allowing for a variation in the number of isolated brine pores; dashed line – predicted thermal conductivity assuming all a single isolated brine pocket; measured data are solid dots – Pringle et al. (2007), diamonds – Nazintsev (1964); crosses – Lewis (1967).

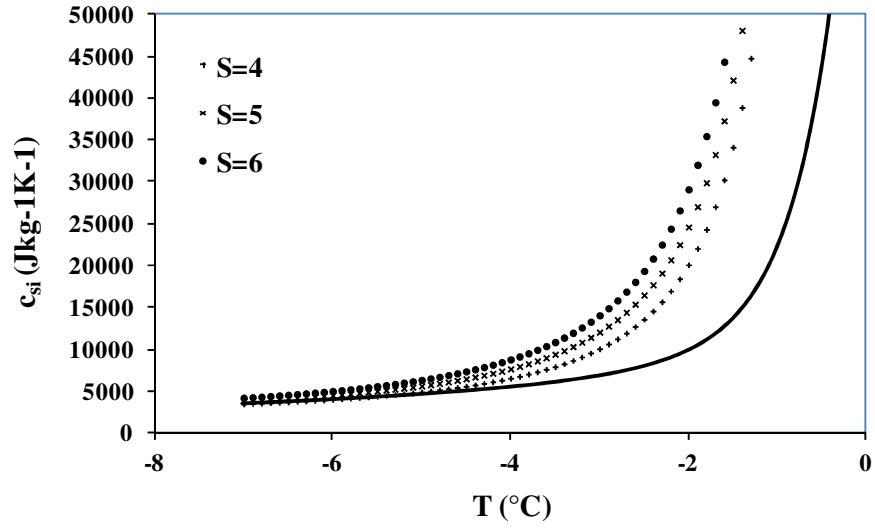


Figure 4: Variation of specific heat capacity with temperature predicted by the microstructural model. Also shown are the parametrizations of Ono (1967), based on field measurements, for ice salinities of 4, 5 and 6 ‰.

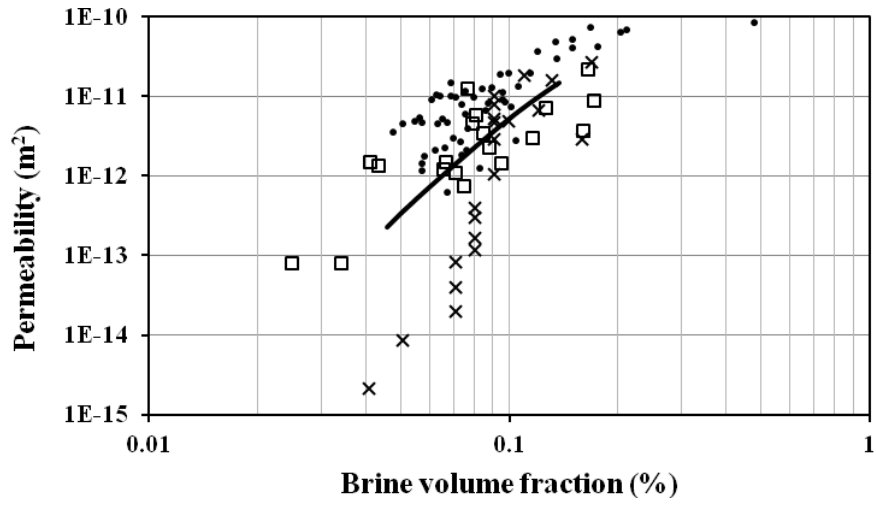


Figure 5: Variation of permeability with brine volume fraction predicted by the microstructural model compared to measured values. Data are as given by Petrich et al. (2006): squares – Saeki et al. (1986), crosses – Ono & Kasai (1985), Saito & Ono (1978), scaled by Maksym & Jefries (2000), dots – Cox & Weeks (1975).



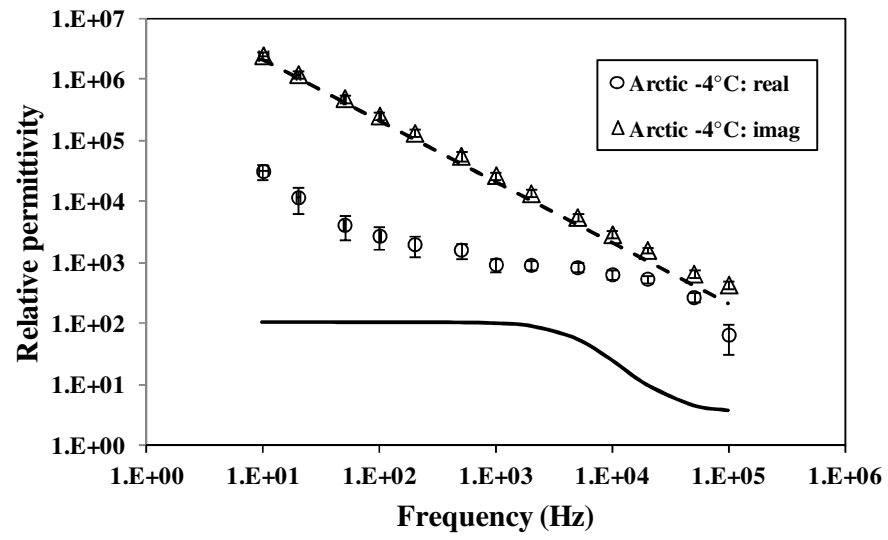


Figure 6: Variation of the horizontal component of the relative dielectric permittivity with frequency predicted by the microstructural model compared to measured values.